Synthesis and Comparative Study of Iron Triad $M(CO)_4(\eta^2$-alkyne) Complexes (M = Fe, Ru, Os; Alkyne = Bis(trimethylsilyl)acetylene)[1]

Richard G. Ball, Michael R. Burke, and Josef Takats*

Department of Chemistry and Structure Determination Laboratory, University of Alberta, Edmonton, Alberta, Canada T6G 2G2

Received December 18, 1986

Photolysis ($\lambda \geq 370$ nm) of $Os_3(CO)_{12}$ (**1c**) with a high intensity irradiation source (500 W) in the presence of bis(trimethylsilyl)acetylene gave, in moderate yield, the first simple mononuclear carbonyl–alkyne complex of osmium, $Os(CO)_4(\eta^2$-$Me_3SiC_2SiMe_3)$ (**2c**). The X-ray molecular structure of **2c** (orthorhombic, $P2_12_12_1$, $a = 13.391$ (3) Å, $b = 13.871$ (3) Å, $c = 9.879$ (3) Å, $Z = 4$; $R = 0.030$, $R_w = 0.037$ for 2073 reflections with $I > 3\sigma(I)$) verified the expected trigonal-bipyramidal disposition of the ligands but with distinct bending of the axial carbonyl groups toward the equatorial alkyne moiety. Involvement from the second full $\pi_\perp$ MO of the alkyne in the bonding is presented as a plausible reason for the distortion. The analogous Ru compound was obtained from in situ prepared $Ru(CO)_5$ and completed the series of iron triad complexes $M(CO)_4(\eta^2$-$Me_3SiC_2SiMe_3)$ (M = Fe, Ru, Os). Comparisons of the stability sequence and spectroscopic properties of the complexes, including ΔG^* for carbonyl group scrambling from variable-temperature ^{13}C NMR studies, indicate that both σ and π components are of import in determining the strength of the M–(η^2-alkyne) interaction.

Introduction

Although the photochemistry of the trinuclear carbonyl complexes of $M_3(CO)_{12}$ (M = Ru, **1b**; M = Os, **1c**) has generated a number of quantitative investigations concerning the mechanism of the photofragmentation process,[2] the photoreactivity of these compounds as a synthetic tool has remained substantially unexplored.[3] Recently, we have reported the photoreaction of **1c** with alkenes[4] which lead, in a straightforward manner, to interesting 1,2-diosmacycles. The synthesis can be extended to a variety of alkenes; however, the corresponding reaction with alkynes gave only three examples of alkyne-bridged species and only in low yields.[5] Equally, mononuclear alkyne–tetracarbonyl derivatives of osmium and ruthenium have escaped preparation under similar reaction conditions.[6] This last result is perhaps not surprising in view of the paucity of simple η^2-alkyne complexes of the iron triad transition-metal carbonyls.[7]

Here we wish to report that by utilizing the bulky bis(trimethylsilyl)acetylene ($Me_3SiC_2SiMe_3$, BTMSA) and somewhat modified reaction conditions the synthesis of "classical" osmium and ruthenium carbonyl–alkyne complexes $M(CO)_4(\eta^2$-$Me_3SiC_2SiMe_3)$ (M = Ru, **2b**; M = Os, **2c**) becomes accessible for the first time. This, together with the previously available iron analogue,[7a] enabled us to carry out a detailed triad comparison of these compounds. As well, the molecular structure of **2c** was determined to provide benchmark parameters for this type of molecule.

Experimental Section

All synthetic procedures were carried out under purified nitrogen or argon atmosphere by using standard Schlenk techniques. Solvents were distilled before use from appropriate drying agents. Bis(trimethylsilyl)acetylene (BTMSA) was purchased from Aldrich Chemical Co. and used without further purification. $Fe_2(CO)_9$ (Alfa Products) and hydrated ruthenium chloride (Engelhard Industries) were used as received. A loan of OsO_4 was provided by Johnson-Matthey, Inc. $Ru_3(CO)_{12}$[8] and $Os_3(CO)_{12}$[9] were prepared by published procedures.

^{13}CO (99% ^{13}C) was purchased from Isotec, Inc. The metal carbonyls were enriched in ^{13}CO either via literature methods ($Fe(^{13}CO)_5$[10] and $Os_3(^{13}CO)_{12}$[11]) or via adaptation of the osmium procedure in the case of $Ru_3(^{13}CO)_{12}$ (toluene solvent, 70 °C for 12 h, and 40 psi of ^{13}CO).

Infrared spectra were obtained on a Nicolet MX-1 Fourier transform spectrometer over the range 2200–1600 cm^{-1}. NMR tubes were sealed under vacuum, and variable-temperature ^{13}C NMR spectra were collected on a Bruker WP-400 spectrometer. An AEI MS-12 spectrometer operating at 70 eV provided mass spectral data. Elemental analyses were carried out by the Microanalytical Laboratory of this Department.

Synthesis of $Os(CO)_4(\eta^2$-$Me_3SiC_2SiMe_3)$ (2c). A 200-mL Schlenk tube (5.0 × 15.0 cm) was charged with 203.5 mg (0.224

(1) A preliminary report was presented at the 69th Canadian Chemical Conference, Saskatoon, Saskatchewan, June 1986, Abstract, IN-E2-2.
(2) (a) Austin, R. G.; Paonessa, R. S.; Giordano, P. J.; Wrighton, M. S. *Adv. Chem. Ser.* **1978**, *No. 168*, 189. (b) Tyler, D. R.; Altobelli, M.; Gray, H. B. *J. Am. Chem. Soc.* **1980**, *102*, 3022. (c) Malito, J.; Markiewicz, S.; Poë, A. *Inorg. Chem.* **1982**, *21*, 4337. (d) Desrosiers, M. F.; Ford, P. C. *Organometallics* **1982**, *1*, 1715. (e) Desrosiers, M. F.; Wink, D. A.; Trautman, R.; Friedman, A. E.; Ford, P. C. *J. Am. Chem. Soc.* **1986**, *108*, 1917. (f) Poë, A. J.; Sekhar, C. V. *J. Am. Chem. Soc.* **1986**, *108*, 3673.
(3) (a) Cotton, F. A.; Deeming, A. J.; Josty, P. L.; Ullah, S. S.; Domingos, A. J. P.; Johnson, B. F. G.; Lewis, J. *J. Am. Chem. Soc.* **1971**, *93*, 4624. (b) Bryan, E. G.; Burrows, A. L.; Johnson, B. F. G.; Lewis, J.; Schiavon, G. M. *J. Organomet. Chem.* **1977**, *129*, C19. (c) Zobl-Ruh, S.; von Philipsborn, W. *Helv. Chim. Acta* **1980**, *63*, 773. (d) Grevels, F.-W.; Reuvers, J. G. A.; Takats, J. *J. Am. Chem. Soc.* **1981**, *103*, 4069. (e) Grevels, F.-W.; Reuvers, J. G. A.; Takats, J. *Angew. Chem.* **1981**, *93*, 475; *Angew. Chem., Int. Ed. Engl.* **1981**, *20*, 452.
(4) Burke, M. R.; Takats, J.; Grevels, F.-W.; Reuvers, J. G. A. *J. Am. Chem. Soc.* **1983**, *105*, 4092.
(5) (a) Burke, M. R.; Takats, J. *J. Organomet. Chem.* **1986**, *302*, C25. (b) Subsequent to (a) both diphenylacetylene and hexafluoro-2-butyne derivatives have been identified from the photochemical preparations.
(6) See ref 4, footnote 5.
(7) For M = Fe see: (a) Pannell, K. H.; Crawford, G. M. *J. Coord. Chem.* **1973**, *2*, 251. For M = Ru see: (b) Cavit, B. E.; Grundy, K. R.; Roper, W. R. *J. Chem. Soc., Chem. Commun.* **1972**, 60. (c) Lehmann, H., Schlenk, K. J.; Chapuis, G.; Ludi, A. *J. Am. Chem. Soc.* **1979**, *101*, 6197. For M = Os see: (d) Burt, R.; Cooke, M.; Green, M. *J. Chem. Soc. A* **1970**, 2981. (e) Segal, S. A.; Johnson, B. F. G. *J. Chem. Soc., Dalton Trans.* **1975**, 677.
(8) Eady, C. R.; Jackson, P. F.; Johnson, B. F. G.; Lewis, J.; Malatesta, M. C.; McParthon, M.; Nelson, W. J. H. *J. Chem. Soc., Dalton Trans.* **1980**, 383.
(9) Johnson, B. F. G.; Lewis, J.; Kilty, P. A. *J. Chem. Soc. A* **1968**, 2859.
(10) Darensbourg, D. J.; Walker, N.; Darensbourg, M. Y. *J. Am. Chem. Soc.* **1980**, *102*, 1213.
(11) Clauss, A. D.; Tachikawa, M.; Shapley, J. R.; Pierpont, C. G. *Inorg. Chem.* **1981**, *20*, 1528.

0276-7333/87/2306-1918$01.50/0

mmol) of $Os_3(CO)_{12}$ (1c), 5.00 mL (3.76 g, 22.1 mmol) of BTMSA, and 100 mL of benzene. The vessel was closed with a serum stopper, photolyzed at room temperature with an Oriel 500-W focussed-beam high-pressure Hg lamp, and filtered with a GWV (Glasswerk Wertheim) cutoff filter ($\lambda \geq 370$ nm), until 1c was completely consumed, ca. 8 h. Solvent and excess BTMSA were removed in vacuo from the resultant yellow-brown solution. A number of X-ray quality crystals could be obtained directly from the residue. Sublimation of the residue (40 °C/0.1 mmHg) onto a dry ice cooled finger gave 143.8 mg (0.304 mmol, 45%) of a yellow powder, mp 49 °C. Due to its volatility some 2c was lost during isolation, thereby reducing the overall isolated yield. Mass spectrum (90 °C, 70 eV); M^+ m/e 474 (^{192}Os), $M^+ - nCO$ (n = 1–4). Anal. Calcd for $C_{12}H_{18}O_4Si_2Os$: C, 30.49; H, 3.84. Found: C, 29.99; H, 3.88. Spectral parameters for this and other compounds are listed in Table II.

Synthesis of $Ru(CO)_4(\eta^2$-$Me_3SiC_2SiMe_3)$ (2b). The synthesis was carried out in two steps with irradiation provided by a Philips HPK 125-W high-pressure Hg lamp kept in a Pyrex immersion well.

(1) A 130-mL Schlenk tube (3.3 × 21.0 cm) was charged with 54.0 mg (0.085 mmol) of $Ru_3(CO)_{12}$ (1b) and 50 mL of pentane. The vessel was closed with a serum stopper. After several freeze–pump–thaw degas cycles, an atmosphere of CO was introduced into the vessel. Long wavelength photolysis ($\lambda \geq 370$ nm, GWV filter) at room temperature produced a clear, colorless solution of $Ru(CO)_5$ in 30 min.

(2) The GWV filter was removed, and the immersion well and the Schlenk tube containing the $Ru(CO)_5$ solution were placed in a dry ice/acetone bath and cooled to ca. −40 °C. The cooling jacket of the well was maintained at low temperature with a Neslab RTE-8 refrigerated circulating bath (methanol coolant). BTMSA (1.00 mL, 0.75 g, 4.42 mmol) was injected through the serum stopper. Photolysis at −40 °C for 2 h resulted in quantitative conversion (by IR) to 2b. Removal of the volatiles (pentane and excess BTMSA) at −25 °C in vacuo gave a yellow powder. Mass spectrum (30 °C, 70 eV): M^+, m/e 384 (^{102}Ru), $M^+ - nCO$ (n = 1–4). The compound is unstable above −20 °C; accordingly elemental analysis could not be performed.

Synthesis of $Fe(CO)_4(\eta^2$-$Me_3SiC_2SiMe_3)$ (2a). The compound was obtained in 41% yield from $Fe_2(CO)_9$ and BTMSA according to the published procedure.[7a]

Synthesis of ^{13}CO-Enriched $M(CO)_4(\eta^2$-$Me_3SiC_2SiMe_3)$. (a) M = Fe. ^{13}CO-enriched 2a was prepared in 39% yield from $Fe(^{13}CO)_5$ and BTMSA under published reaction conditions.[7a] **(b) M = Ru.** $Ru(^{13}CO)_5$ was obtained in situ from $Ru_3(^{13}CO)_{12}$ and ^{13}CO (vide supra) and used subsequently as described above. **(c) M = Os.** Enriched $Os_3(^{13}CO)_{12}$ was used directly as reported above.

X-ray Structure Determination of 2c. Crystal data and general conditions of data collection[12] and structure refinement[13] are given in Table I. A direct methods[14] solution gave the positional parameters for the Os atom with the remaining nonhydrogen atoms located in different Fourier maps after least-squares refinement. Refinement was carried out on F by using weights of $1/\sigma(F_o)$. The neutral atom scattering factors were calculated from the analytical expression for the curves[15] with the f' and f'' components of anomalous dispersion[16] included for all non-H atoms. Reflection data were corrected for absorption by using the method of Walker and Stuart[17] which yielded coefficients for F_o ranging from 0.827 to 1.190. An examination of 37 low-angle intense reflections indicated the data was suffering from secondary extinction effects. Accordingly this parameter was included during the latter stages of the refinement procedure.

All H atoms were included at their idealized positions (calculated by assuming C–H = 0.95 Å and sp^3 geometry) and constrained to "ride" with the attached C atom. They were assigned fixed, isotropic thermal parameters 1.2 times those of the parent C atom.

The initial choice for the enantiomorph was made during the direct methods solution and that this was correct was confirmed by refinement of the inverted model. The inverted model had a final R_2 value of 0.065 which is significantly larger than the corresponding value for the original model.

A probability plot analysis was done on the $\delta(R)$ values ($\delta(R_1) = |F_{o_i}| - |F_{c_i}|/\sigma(R_{o_i})$), and this plot shows a strong deviation from linearity. This analysis confirms the impression, given by the higher than expected estimated standard deviations on the bond distances and angles, that the data are not of the best quality. We ascribe this to the poor quality of the crystals available for use in the diffraction experiment rather than any particular weakness in the structural model.

Table I. Summary of Crystallographic Data

Crystal Parameters	
formula	$C_{12}H_{18}O_4OsSi_2$
fw	472.65
space group	$P2_12_12_1$
a, Å	13.391 (3)
b, Å	13.871 (3)
c, Å	9.879 (3)
V, Å^3	1835
Z	4
D_{calcd}, g cm^{-1}	1.711
μ, cm^{-1}	70.92
no. of 2θ range for reflcns used in cell detrm	24, 17–30°
cryst dimen, mm	0.25 × 0.37 × 0.32
Data Collection and Structure Refinement	
diffractometer	Enraf-Nonius CAD4
radiatn	Mo Kα (0.710 73 Å)
monochromator	graphite cryst, incident beam
temp, °C	−20
takeoff angle, deg	3.0
detector aperture, mm	2.40 horiz–4.0 vert.
cryst–detector dist, mm	205
scan type	ω–2θ
scan rate, deg min^{-1}	2.0–10.1
scan width, deg in ω	0.70 + 0.35 tan θ
index range; 2θ limit	h,k,l; 55.00°
reflcns measd	2408 unique
reflcns used	2073 with $I > 3\sigma(I)$
correctns applied	abspn
secondary extinction coeff	1.6×10^{-6}
no. of refined params	173
R_1[a]	0.030
R_2[b]	0.037
GOF[c]	1.04
largest final shift/esd	0.05
diff Fourier, highest peak	0.4 (1)

[a] $R_1 = \sum||F_o| - |F_c||/\sum|F_o|$. [b] $R_2 = [\sum w(|F_o| - |F_c|)^2/\sum wF_o^2]^{0.5}$. [c] GOF $= [\sum w(|F_o| - |F_c|)^2/(N_o - N_v)]^{0.5}$.

Results and Discussion

Synthesis and Characterization of $M(CO)_4(\eta^2$-$Me_3SiC_2SiMe_3)$ (M = Ru, 2b; M = Os, 2c). Initial attempts of preparing 2c under previously described photochemical conditions[5] (125-W light source) resulted in little overall reaction even after long irradiation periods.[18] Resorting to a higher intensity light source (see Experimental Section), the reaction of 1c with BTMSA went to completion after 8 h to afford a 45% isolated yield of an air-stable, volatile yellow solid (eq 1). Elemental analysis

(12) The diffractometer used for data collection is an Enraf-Nonius CAD4F with an FTS Systems air-jet crystal cooler. The diffractometer programs used are those supplied by Enraf-Nonius with some local modifications and additions.

(13) The computer programs used in this analysis include the Enraf-Nonius Structure Determination Package by B.A. Frenz (*Computing in Crystallography*; Delft University Press: Delft, Holland, 1978; pp 64–71) and several locally written or modified programs.

(14) Main, P.; Lessinger, L.; Woolfson, G.; Declercq, J. P., MULTAN 11/82.

(15) *International Tables for X-Ray Crystallography*; Kynoch Press: Birmingham, England; 1974; Vol. IV, Table 2.2B.

(16) Reference 15, Table 2.3.1.

(17) Walker, N.; Stuart, D. *Acta Crystallogr., Sect. A: Found. Crystallogr.* **1983**, *A39*, 158.

(18) Mass spectral analysis of the crude reaction residue gave some indication for the formation of 2c.

Table II. Spectral Data for $M(CO)_4(\eta^2\text{-}Me_3SiC_2SiMe_3)$

M	IR,[a] cm^{-1} ν_{CO}		ν_{CC}	^{13}C NMR[b] T, °C	δ_{CO}	T, °C	δ_{CO}[c]	δ_{CSiMe_3}	δ_{CSiMe_3}
Fe, **2a**	2078 (w)	2003 (vs)	1875 (w)	−64	214.1	−92	216.2	87.8	−1.4
	1998 (m)	1969 (s)					211.9		
Ru, **2b**	2097 (w)	2019 (vs)	1860 (w)	−50	201.5	−80	205.9	89.5	−1.1
	2006 (m)	1981 (s)					198.8		
Os, **2c**	2099 (w)	2016 (vs)	1809 (w)	+10	183.2	−40	186.4	92.7	−0.9
	2003 (m)	1976 (s)					179.8		

[a] In pentane solution. Abbreviations: w, weak; m, medium; s, strong; vs, very strong. [b] In CD_2Cl_2 solution at 100.6 MHz. Chemical shifts in ppm from Me_4Si. [c] The two signals at low temperatures are in the ratio 1:1.

and spectroscopic characterization (vide infra) confirm the formulation as **2c**, the first simple mononuclear carbonyl–alkyne complex of osmium.

$$\underset{\mathbf{1c}}{Os_3(CO)_{12}} + \text{excess BTSMA} \xrightarrow[\text{benzene, 40 °C, 8 h}]{\lambda > 370 \text{ nm}, 450 \text{ W}} 3\underset{\mathbf{2c}}{Os(CO)_4(\eta^2\text{-BTMSA})} \quad (1)$$

Attempts to prepare the analogous ruthenium compound under similar conditions met with failure. Photolysis of $Ru_3(CO)_{12}$ (**1b**) and excess BTMSA in benzene resulted only in precipitation of the orange-red insoluble, polymeric form of ruthenium carbonyl.[2e,19] However, application of the metal pentacarbonyl route previously used to prepare the iron complex **2a**[7a] proved to be highly satisfactory. Photolysis of in situ prepared $Ru(CO)_5$[20] and excess BTMSA at −40 °C gave, after 2 h, quantitative conversion (by IR monitoring) to **2b** (eq 2). Removal of

$$\underset{\mathbf{1b}}{Ru_3(CO)_{12}} \xrightarrow[\text{pentane, } \lambda > 370 \text{ nm}]{\text{CO (1 atm), room temp}} 3Ru(CO)_5 \quad (2)$$

$$Ru(CO)_5 + \text{excess BTMSA} \xrightarrow[\text{pentane, } \lambda > 280 \text{ nm}]{-40 \text{ °C, 2 h}} \underset{\mathbf{2b}}{Ru(CO)_4(\eta^2\text{-BTMSA})}$$

the volatiles at −25 °C left behind pure **2b** as a yellow solid, which is stable only below −20 °C. A mass spectrum of **2b** could be obtained and showed, like **2c**, the parent molecular ion followed by the successive loss of four carbonyl moieties. Further confirmation of the molecular formulation was obtained from spectroscopic data on **2b** and **2c** (Table II). In the infrared spectrum of the molecules,[21] the position and intensity distribution of the four terminal carbonyl stretching bands (ν_{CO}) are fully consistent with the alkyne ligand occupying an equatorial position of a trigonal-bipyramidal structure. Also, weak absorptions in the 1800–1900 cm^{-1} region can be attributed to the carbon–carbon stretching modes (ν_{CC}) of the complexed alkyne. The low-temperature ^{13}C NMR spectra show two equally intense signals, one each for the equivalent axial and equatorial carbonyl ligands of *eq*-$M(CO)_4(\eta^2\text{-BTMSA})$ of C_{2v} symmetry.

Molecular Structure of 2c. In order to substantiate the molecular geometry of compounds **2** as suggested by the spectroscopic data, an X-ray structure analysis of **2c** was carried out. Figure 1 shows a perspective view of the molecule with the atom numbering scheme. Table III gives a listing of the final atomic and thermal parameters, and relevant bond distances and angles are collected in Table IV.

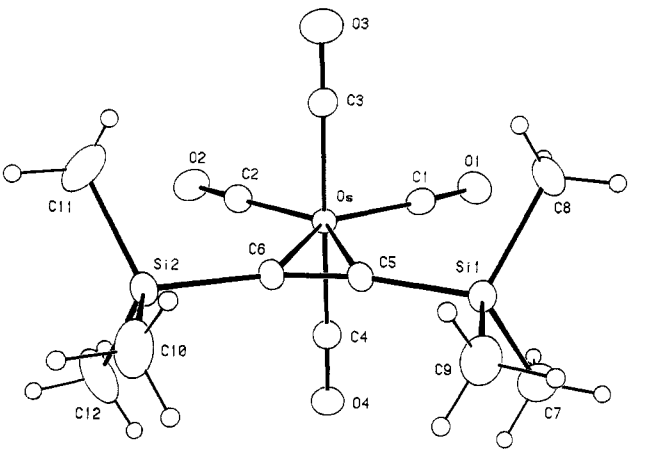

Figure 1. Perspective view of $Os(CO)_4(\eta^2\text{-}Me_3SiC_2SiMe_3)$ (**2c**) showing the atom numbering scheme. Atoms are represented by thermal ellipsoids at the 20% probability level except for the H atoms which are drawn at an arbitrary size.

Table III. Positional (×10³) and Isotropic Thermal (×10²) Parameters for $Os(CO)_4(\eta^2\text{-}Me_3SiC_2SiMe_3)$ (2c)[a]

atom	x	y	z	U, Å²
Os	358.20 (2)	115.43 (2)	201.58 (2)	3.805 (5)
Si(1)	617.4 (1)	126.6 (1)	75.4 (2)	4.35 (5)
Si(2)	507.3 (1)	125.7 (1)	520.7 (2)	4.56 (5)
O(1)	295.6 (5)	114.2 (4)	−94.9 (5)	8.1 (2)
O(2)	168.8 (4)	107.5 (4)	372.7 (7)	8.0 (2)
O(3)	364.6 (4)	336.6 (4)	210.4 (6)	8.1 (2)
O(4)	390.1 (5)	−105.8 (4)	205.4 (6)	7.6 (2)
C(1)	320.0 (5)	114.7 (5)	14.7 (7)	5.4 (2)
C(2)	239.5 (5)	108.5 (5)	311.1 (7)	5.3 (2)
C(3)	361.3 (5)	255.0 (5)	206.4 (8)	5.4 (2)
C(4)	375.9 (4)	−24.5 (5)	203.7 (8)	4.8 (2)
C(5)	527.0 (5)	123.0 (4)	214.2 (6)	4.3 (2)
C(6)	493.6 (4)	123.1 (4)	334.9 (6)	4.1 (2)
C(7)	606.7 (6)	14.2 (6)	−25.5 (9)	7.4 (3)
C(8)	588.4 (6)	233.5 (6)	−30.1 (8)	6.5 (3)
C(9)	744.0 (6)	137.7 (7)	149.4 (9)	7.1 (3)
C(10)	641.6 (6)	138.7 (7)	560.5 (8)	7.2 (3)
C(11)	437.0 (7)	231.5 (8)	582 (1)	10.2 (4)
C(12)	457.6 (8)	12.1 (8)	588 (1)	10.9 (4)

[a] The equivalent isotropic thermal parameter is given by $U = {}^1/_3\Sigma r_i^2$ where r_i are the root-mean-square amplitudes of vibration.

The view clearly shows the trigonal-bipyramidal arrangement of the ligands around osmium, with the alkyne carbon atoms lying in the equatorial plane (torsional angles C(1)–Os–C(5)–C(6) = −178.5° and C(2)–Os–C(6)–C(5) = 178.6°). The stereochemistry of the molecule parallels that observed in $M(CO)_4(\eta^2\text{-olefin})$ (M = Fe,[22] Ru[23]) derivatives

(19) Hastings, W. R.; Baird, M. C. *Inorg. Chem.* **1986**, *25*, 2913.
(20) Johnson, B. F. G.; Lewis, J.; Twigg, M. W. *J. Organomet. Chem.* **1974**, *67*, C75.
(21) Solution IR of **2c** can be obtained without any undue precaution. However **2b**, like many other $Ru(CO)_4(\eta^2\text{-olefin})$ complexes,[3d] is labile in solution. Solution samples for IR analysis must be stabilized by the addition of a small amount of free BTMSA; otherwise back reaction to **1b** occurs rapidly.
(22) Cotton, F. A.; Lahuerta, P. *Inorg. Chem.* **1975**, *14*, 110.

Table IV. Selected Bond Distances and Angles for $Os(CO)_4(\eta^2$-$Me_3SiC_2SiMe_3)$ (2c)

	Bond Distances (Å)		
Os–C(1)	1.916 (7)	C(1)–O(1)	1.130 (9)
Os–C(2)	1.925 (8)	C(2)–O(2)	1.125 (9)
Os–C(3)	1.937 (7)	C(3)–O(3)	1.133 (8)
Os–C(4)	1.955 (7)	C(4)–O(4)	1.143 (8)
Os–C(5)	2.267 (6)	Si(1)–C(5)	1.829 (7)
Os–C(6)	2.244 (6)	Si(2)–C(6)	1.845 (6)
C(5)–C(6)	1.273 (8)	Si(1)–C(Me)	1.854 (9)
		Si(2)–C(Me)	1.850 (10)
	Bond Angles (deg)		
C(1)–Os–C(2)	108.8 (3)	Os–C(1)–O(1)	178.6 (8)
C(1)–Os–C(3)	92.0 (3)	Os–C(2)–O(2)	177.4 (8)
C(1)–Os–C(4)	92.1 (4)	Os–C(3)–O(3)	178.8 (7)
C(1)–Os–C(5)	108.6 (3)	Os–C(4)–O(4)	177.4 (6)
C(1)–Os–C(6)	141.4 (4)		
C(2)–Os–C(3)	93.1 (3)	Os–C(5)–Si(1)	128.3 (3)
C(2)–Os–C(4)	92.6 (3)	Os–C(5)–C(6)	72.6 (8)
C(2)–Os–C(5)	142.6 (3)	Si(1)–C(5)–C(6)	159.1 (6)
C(2)–Os–C(6)	109.9 (3)	Os–C(6)–Si(2)	131.5 (3)
C(3)–Os–C(4)	171.6 (3)	Os–C(6)–C(5)	77.6 (4)
C(3)–Os–C(5)	86.1 (3)	Si(2)–C(6)–C(5)	153.7 (6)
C(3)–Os–C(6)	85.5 (3)		
C(4)–Os–C(5)	85.6 (3)		
C(4)–Os–C(6)	86.7 (3)		
C(5)–Os–C(6)	32.8 (2)		

and conforms to the electronic site preference arguments presented by Hoffmann.[24] It also closely resembles the only other structurally characterized $M(CO)_4(\eta^2$-alkyne) fragment encountered in $Fe_2(CO)_8(Ph_2PC{\equiv}C$-*t*-Bu).[25] The average Os–CO(axial) (1.946 (7) Å) and Os–CO(equatorial) (1.921 (8) Å) bond distances are marginally different. The shorter Os–CO(equatorial) bonds indicate that the BTMSA ligand is a poorer π-acid than the CO group and allows for greater back-bonding to the carbonyl moieties from osmium in the equatorial plane than toward the axial carbonyls. Similar differences between axial and equatorial carbonyl groups have been observed in the previously mentioned iron complex (1.832 (3) and 1.807 (9) Å) and in *eq*-$Os(CO)_4(SbPh_3)$ (1.946 (6) and 1.918 (7) Å).[26]

The strength of the metal–alkyne interaction can be assessed with the aid of structural parameters, i.e., C–C bond distance, the back-bending angle of the alkyne substituents, and the metal–C(alkyne) bond length.[27] In **2c**, the C(5)–C(6) bond length is 1.273 (8) Å which lies midway between the accepted values for C–C double and triple bonds.[28] This distance compares favorably with 1.275 (7) Å observed in $Fe_2(CO)_8(Ph_2PC{\equiv}C$-*t*-Bu)[25] and with those obtained for a number of zerovalent, trigonal nickel alkyne complexes.[29] The back-bending angles of the $SiMe_3$ moieties at C(5) (20.9 (6)°) and C(6) (26.3 (6)°) are somewhat smaller than those in the above-mentioned complexes (27° and 30° in Fe and 27–31° in Ni). Taken together with the length of the C–C bond, this indicates slight changes in the relative importance of the retrodative Os–alkyne interaction in **2c** compared to the first-row transition-metal complexes.

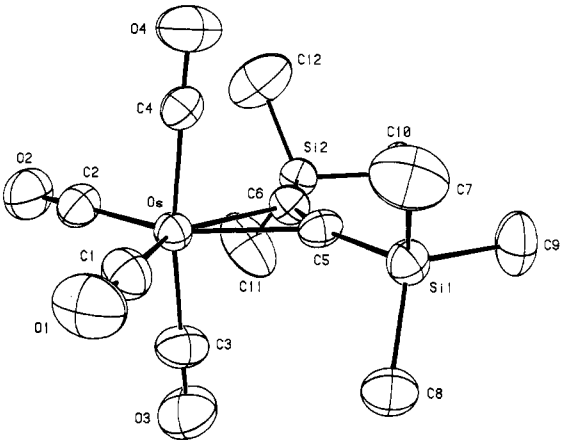

Figure 2. View of **2c** emphasizing the bending of the axial carbonyl groups toward the equatorial alkyne moiety.

Chart I

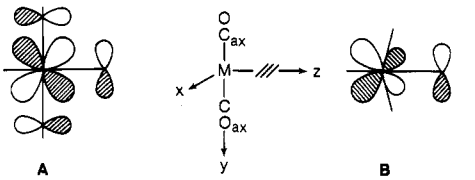

It is interesting to note that the $SiMe_3$ moieties are eclipsed in **2c**. Therefore the interactions between the two silyl groups appear to be less important than those between a methyl group and an equatorial CO ligand which would result from a staggered orientation of the $SiMe_3$ groups. As it is, the Os–CO(equatorial) bond axis lies along the favorable Me–Si–Me angle bisector.

A direct comparison of the Os–C(alkyne) distances in **2c** with other simple $Os(\eta^2$-alkyne) fragments is not possible. However, as expected, these bond lengths (Os–(C5) = 2.267 (6) Å and Os–C(6) = 2.244 (6) Å) are longer than those observed in alkyne-bridged polynuclear derivatives. For instance, in $Os_2(CO)_8(\mu$-η^1,η^1-DMAD)[5] (DMAD = dimethyl acetylenedicarboxylate) which contains a parallel alkyne bridge, the two Os–C(alkyne) σ-bonds are 2.138 (5) Å. Whereas, in $Os_3(CO)_{10}(C_2Ph_2)$,[30] the bridging alkyne unit displays two Os–C σ-bonds of 2.182 (8) and 2.070 (9) Å and two Os–C π-interactions of 2.188 (8) and 2.293 (9) Å. Consistent with the stronger osmium–alkyne interaction in these bridged species, the C–C bond lengths, 1.33 (1) and 1.439 (10) Å respectively, are longer than those in **2c**.

A final point of interest of the present structure is the distinct, if not severe, bending of the axial carbonyl groups toward the equatorial alkyne moiety. A clear view of this is provided in Figure 2. The C(3)–Os–C(4) angle is 171.6 (3)°. Interestingly, a similar type of distortion, with only a slightly different canting angle of 173.5 (2)°, has been observed also in the Fe–(η^2-alkyne) complex $Fe_2(CO)_8$-$(Ph_2PC{\equiv}C$-*t*-Bu).[25] Since the latter compound presents a different type of alkyne ligand and crystal environment to the iron center, we tend to dismiss packing forces and believe that electronic factors are at the origin of the bending of the axial carbonyl groups. Clearly the effects of the second set of π MO's on the alkyne unit ($\pi_\perp$ and/or $\pi_\perp^*$) must be scrutinized in this regard. In support of the probable involvement of the extra set of orbitals is the observation that in related $M(CO)_4(\eta^2$-alkene) complexes the CO_{ax}–M–CO_{ax} angle is very close to 180° and often the

(23) Ball, R.; Gagné, M.; Takats, J., manuscript in preparation.
(24) Allbright, T. A.; Hoffmann, R.; Thibeault, J. C.; Thorn, D. L. *J. Am. Chem. Soc.* **1979**, *101*, 3801.
(25) Carty, A. J.; Smith, W. F.; Taylor, N. J. *J. Organomet. Chem.* **1978**, *146*, C1.
(26) Martin, L. R.; Einstein, F. W. B.; Pomeroy, R. K. *Inorg. Chem.* **1985**, *24*, 2777.
(27) Ittel, S. D.; Ibers, J. A. *Adv. Organomet. Chem.* **1976**, *14*, 33.
(28) *International Tables for X-ray Crystallography*; Kynoch Press: Birmingham, England, 1974; Vol. III, Table 4.2.2.
(29) Davies, B. W.; Payne, N. C. *Inorg. Chem.* **1974**, *13*, 1848.
(30) Pierpont, C. G. *Inorg. Chem.* **1977**, *16*, 636.

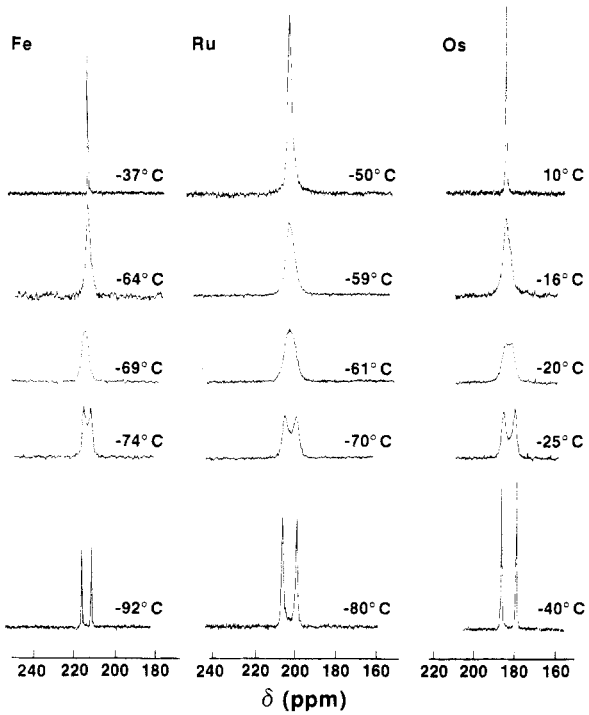

Figure 3. Variable-temperature ^{13}C NMR spectra of $M(CO)_4(\eta^2\text{-}Me_3SiC_2SiMe_3)$ compounds.

axial CO groups bend slightly away from the equatorial olefin.[31]

Focusing on the $Os(CO_{ax})_2(\eta^2\text{-alkyne})$ fragment, Chart I shows the orbitals of interest. The choice of axis system and orbital designations follow the development by Hoffmann.[24] Only the combination which results in positive overlap between metal d_{yz} (b_1), CO_{ax} (π_{yz}^*), and acetylene $\pi_\perp$ orbitals is shown in A. Since the equatorial CO groups also compete, via back-bonding, for the electron density in the metal d_{yz} orbital, the axial carbonyl ligands by moving slightly toward the alkyne $\pi_\perp$ orbital may compensate for this competition. Of course in the present context with both metal d_{yz} and alkyne $\pi_\perp$ orbitals being full, this is a four-electron interaction and the antibonding combination between these two orbitals will also contain an electron pair. However, movement of axial CO groups toward the equatorial alkyne results in a "rehybridization" of d_{yz} as shown in B, which should reduce the two-electron repulsion between d_{yz} and $\pi_\perp$ and in addition increases the π-back-bonding to the equatorial CO groups as well. Although symmetry considerations allow for possible overlap between metal d and alkyne $\pi_\perp^*$ orbitals, we think this to be of minor importance and not readily adapted to account for the kind of axial carbonyl groups movement seen in these molecules.

The importance of the second full MO of alkynes ($\pi_\perp$) in electron-deficient mononuclear complexes is well-recognized, and the alkyne is viewed as a "four-electron" donor unit.[32] Additional interactions are also seen in binuclear complexes containing perpendicular alkyne-bridging moieties[33] and in situations where the alkyne is bridging

Scheme I

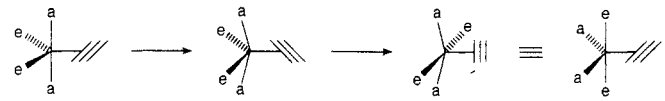

Table V. Comparative Spectroscopic and Energetic Data on $M(CO)_4(\eta^2\text{-}Me_3SiCCSiMe_3)$ (2)

M	$\Delta(\nu_{CC})$,[a] cm^{-1}	$\Delta(\delta_{C_{alk}})$,[b] ppm	$\Delta G^*_{T_c}$,[c] kcal/mol	T_c, °C
Fe	233	25.2	9.0	−69
Ru	248	23.5	9.5	−54
Os	299	20.3	11.0	−20

[a] $\Delta(\nu_{CC}) = \nu_{CC}$ (free BTMSA) − ν_{CC} (complexed BTMSA), ν_{CC} (free BTMSA) = 2108.[35] [b] $\Delta(\delta C_{alk}) = \delta(CSiMe_3$, free) − $\delta(CSiMe_3$, complexed), $\delta(CSiMe_3$, free) = 113.0.[36] [c] Free energies of activation at the coalescence temperature, T_c, were calculated by using the approximate expression application to the coalescence of two equal singlets.[37]

three metal centers via a $2\sigma + \pi$ binding mode, as in $Os_3(CO)_{10}(C_2Ph_2)$[30] and related compounds.[33] It appears from the present observation and analysis that under appropriate circumstances even electron-precise compounds may involve the $\pi_\perp$ MO of the coordinated alkyne. It would be of interest to establish both experimentally and theoretically how the nature of the alkyne and of the transition-metal effects the magnitude of this involvement.

Variable-Temperature ^{13}C NMR Behavior. The variable-temperature ^{13}C NMR spectra of compounds **2** are shown in Figure 3. As expected from the well-known behavior of the related $M(CO)_4(\eta^2\text{-olefin})$ complexes,[33] the tetracarbonyl–alkyne complexes are fluxional as well. At the low-temperature limit, consistent with the solid-state structure of **2c**, each spectrum exhibits two signals of equal intensity in the carbonyl region. The simplicity of the spectra and the observation that in $M(CO)_4(\eta^2\text{-olefin})$ complexes axial carbonyl groups may resonate both at higher[33a,e] and at lower[33c,d] fields than the equatorial carbonyl moieties preclude unambiguous assignment of the resonances of compounds **2**. As the temperature is raised, the resonances broaden, coalesce, and emerge as single sharp signals at the expected averaged positions. The high-temperature-limiting, sharp singlet could not be observed for the ruthenium derivative due to its instability in solution much above −50 °C. The observed line-shape changes are temperature reversible and independent of concentration and of added free alkyne. This establishes that the scrambling of the axial and equatorial carbonyl groups is intramolecular and proceeds without dissociation of the equatorial alkyne ligand. Although mechanistic delineation of the exchange process is negated by the simplicity of the coalescence pattern, an attractive possibility is the coupled alkyne rotation–Berry pseudorotation which is operationally identical with the well established, although not exclusive,[33c,d] coupled olefin rotation–carbonyl exchange process in the related $M(CO)_4(\eta^2\text{-olefin})$ complexes.[33a,b,e] Free energies of activation have been calculated (Table V). Discussion of the observed

(31) (a) Cotton, F. A.; Lahuerta, P. *Inorg. Chem.* **1975**, *14*, 116: $Fe(CO)_4(\eta^2\text{-acenaphtalene})$, $CO_{ax}\text{–}Fe\text{–}CO_{ax}$ = 178.7 (1)°. (b) Chisnall, B. M.; Green, M.; Hughes, R. P.; Wells, A. J. *J. Chem. Soc., Dalton Trans.* **1976**, 1899: $Fe(CO)_4(\eta^2\text{-furanone})$, $CO_{ax}\text{–}Fe\text{–}$(midpoint olefin) = 91.7 (3) and 90.2 (3)°.

(32) (a) Tatsumi, K.; Hoffmann, R.; Templeton, J. *Inorg. Chem.* **1982**, *21*, 466. (b) Morrow, J. R.; Tonker, T. L.; Templeton, J. L. *J. Am. Chem. Soc.* **1985**, *107*, 6956.

(33) Sappa, E.; Tiripicchio, A.; Braunstein, P. *Chem. Rev.* **1983**, *83*, 203.

(34) For M = Fe see: (a) Kruczynski, L.; LiShingMan, L. K. K.; Takats, J. *J. Am. Chem. Soc.* **1974**, *96*, 4006. (b) Wilson, S. T.; Coville, N. J.; Shapley, J. R.; Osborn, J. *J. Am. Chem. Soc.* **1974**, *96*, 4038. (c) von Büren, M.; Cosandey, M.; Hansen, H.-J. *Helv. Chim. Acta* **1980**, *63*, 738. (d) Cosandey, M.; von Büren, M.; Hansen, H.-J. *Helv. Chim. Acta* **1983**, *66*, 1. For M = Ru see: (e) Kruczynski, L.; Martin, J. L.; Takats, J. *J. Organomet. Chem.* **1974**, *86*, C9 and ref 3d. For M = Os see: (f) Rushman, P.; van Buuren, G. N.; Shiralian, M.; Pomeroy, R. K. *Organometallics* **1983**, *2*, 693 and ref 4.

(35) Kriegsman, H.; Beyer, H. *Z. Anorg. Allg. Chem.* **1961**, *311*, 180.

(36) Wrackmeyer, B. *J. Organomet. Chem.* **1979**, *166*, 353.

(37) Kost, D.; Carlson, E. H.; Raban, M. *J. Chem. Soc. D* **1971**, 656.

trend is deferred to the next section.

Triad Comparison of $M(CO)_4(\eta^2$-$Me_3SiC_2Me_3$) Compounds and Nature of the M–(η^2-Alkyne) Interaction. The bonding, structure, and reactivity of transition-metal complexes are under the influence of numerous and often subtly interdependent factors. To gauge the hierarchy of importance of these factors is very difficult. However, triad comparison of homologous series of compounds is well-recognized to be extremely valuable in this regard. The observation of metal-dependent trends in properties often clarifies bonding ideas and may serve as a guide for structure and reactivity predictions.

In this section we wish to compare the available data on compounds **2**, especially as they pertain to the major point of interest, the M–(η^2-alkyne) interaction. The relevant spectroscopic and energetic data are compared in Table V.

As usual,[38] metal–alkyne π interaction lowers the C≡C stretching frequency of the alkyne ligand in the complexes. The magnitude of the coordination shift ($\Delta(\nu_{CC})$), albeit substantial especially in **2c**, is still too small to consider the bonding in these compounds as well represented by the metallacyclopropene formulation. This conclusion is further reinforced by the Os–C(alkyne) distances which, vide supra, are significantly longer than those in the corresponding diosmacyclobutene-type compound $Os_2(CO)_8(\mu$-η^1,η^1-DMAD).[5a] The coordination shift increases in the order Fe < Ru ≪ Os and reflects[38,39] a concomitant reduction in C≡C bond order.

Another measure of this bond order reduction is the chemical shift of the coordinated alkyne carbon atoms. Deshielding of the alkyne carbons upon coordination to a metal has been attributed to an increase in the olefinic character of the alkyne as its π-bond order is reduced.[40] Indeed, Templeton[41] has established an empirical relationship between the number of electrons donated by the alkyne and its ^{13}C chemical shifts. Although the progressively lower field shifts of the alkyne carbons ($\delta_{C_{alk}}$) in complexes **2** from Fe to Os[42] (Table I) parallels the variation in $\Delta(\nu_{CC})$ (and indicates reduced C≡C bond order down the triad), the sign and magnitude of the coordination shift require some further comments. Reference to Table V reveals that contrary to previous cases with normal, carbon-substituted alkynes, the coordination shift in complexes **2** is positive (i.e., complexed BTMSA resonates at higher field than the free ligand). We can trace this anomaly not to a suddenly different metal–alkyne bonding in compounds **2** but to the influence of the $SiMe_3$ moiety on the carbon chemical shift in free BTMSA. The chemical shift of the alkyne carbon in free BTMSA is at δ113.0,[36] some 35 ppm to *lower* field than in related carbon substituted alkynes.[44] A major part of this downfield shift has been attributed to the p_π–d_π type conjugative interaction between the C≡C bond and the $SiMe_3$ moiety,[36,45]

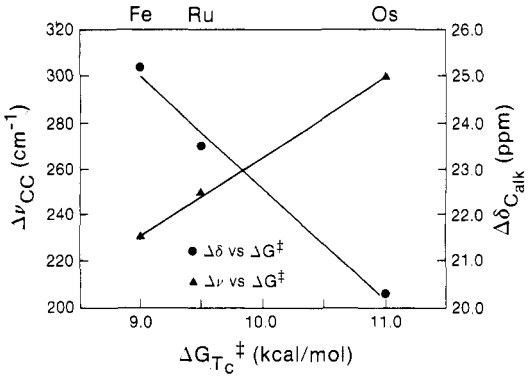

Figure 4. Graphical comparison of the variation in coordination shifts (IR and NMR) vs. $\Delta G^{\ddagger}$ for carbonyl scrambling in compounds **2**.

giving rise to reduced π-bond order in free BTMSA. The situation, of course, is very different in complexes **2** where the bending back of the $SiMe_3$ moieties from the C≡C bond (Figures 1 and 2) greatly reduces this type of interaction. Thus coordination shift calculation in compounds **2** should have as its starting point the chemical shift of the alkyne carbons of "free BTMSA" but in a geometry as seen in **2c** to remove the effect of the C-(p_π)→Si(d_π) interaction. This would result in a movement of the resonance position to significantly higher field than the observed 113 ppm in ground-state BTMSA. Regrettably, the magnitude of this predicted chemical shift is not available, and therefore discussion concerning the absolute magnitude of the observed ^{13}C coordination shifts in compounds **2** would be futile. Nevertheless, we believe that neglect of this "correction term" is indeed the reason for the sign reversal of $\Delta\delta$ and consequently for the trend of decreasing coordination shift in compounds **2** as the triad is descended.[46]

Finally, we wish to consider the trend in the free energies of activation, $\Delta G^{\ddagger}_{T_c}$, for carbonyl group scrambling in these molecules. Although the energetics of the related process in $M(CO)_4(\eta^2$-olefin) (M = Fe, Ru, Os) compounds are not simply dependent on a single variable,[24,47] the available experimental data supports the view that the trends in activation energies are mainly controlled by the π-component of the metal–olefin bond.[34] The same rationale is expected to hold for compounds **2**. The trend of increasing $\Delta G^{\ddagger}$ in the order Fe < Ru < Os mirrors the changes observed in the analogous η^2-olefin compounds and indicates increased metal d to π^*(alkyne/alkene) back-bonding for both classes of compounds as this triad of transition metals is descended. It is noteworthy that the increase in back-bonding from Fe to Ru is apparently more than offset by a concomitant decrease in π(alkyne) to metal d orbital donor interaction since the ruthenium compound is much less stable than its iron analogue. The stability sequence is Os (**2c**) > Fe (**2a**) ≫ Ru (**2b**). It is worth emphasizing that the importance of the σ-component of the metal–alkyne bonding interaction became clear only when the stability of the complexes and the variation in barriers for the coupled alkyne rotation–carbonyl scrambling process were scrutinized together. The successful identification of the individual components of the metal–alkyne bond resides in the fact that the trend in $\Delta G^{\ddagger}$ is uniquely modulated by the π-component of this bond. The coor-

(38) Maslowsky, J. E. *Vibrational Spectra of Organometallic Compounds*; Wiley-Interscience: New York, 1977; pp 248–263.
(39) Greaves, E. O.; Lock, C. J. L.; Maitlis, P. M. *Can. J. Chem.* **1968**, *46*, 3879.
(40) Chisholm, M. H.; Clark, H. C.; Manzer, L. E.; Stothers, J. B. *J. Am. Chem. Soc.* **1972**, *94*, 5087.
(41) Templeton, J. L.; Ward, B. C. *J. Am. Chem. Soc.* **1980**, *102*, 3288.
(42) It is interesting to note that this shift to lower field of the bound alkyne carbons as the metal is changed from Fe → Ru → Os in this series of isostructural complexes occurs despite the well-established *upfield* ^{13}C "metal shift" down a transition-metal triad.[43] In other words, it appears that the change in M–alkyne interaction in compounds **2** is in fact capable of offsetting the metal shifts.
(43) Mann, B. E.; Taylor, B. F. *^{13}C NMR Data for Organometallic Compounds*; Academic: New York, 1981.
(44) Stothers, J. B. *Carbon-13 NMR Spectroscopy*; Academic: New York, 1972; pp 85–90.
(45) Adridge, C. J. *Organomet. Chem. Rev., Sect. A* **1970**, *5*, 323.
(46) In other words a smaller positive $\Delta\delta$, after "correction", would translate into a larger negative $\Delta\delta$.
(47) (a) Demuynck, J.; Strich, A.; Veillard, A. *Nouv. J. Chim.* **1977**, *1*, 217. (b) Axe, F. U.; Maynick, D. S. *J. Am. Chem. Soc.* **1984**, *106*, 6230.

dination shifts $\Delta(\nu_{CC})$ and $\Delta(\delta_{C_{alk}})$ indicate variations in C≡C bond order and therefore reflect composite changes in forward donation and back acceptance from the alkyne moiety. To further probe the relative importance of these two factors on the coordination shifts, the variations in $\Delta(\delta_{C_{alk}})$ vs. $\Delta G^{\ddagger}$ and $\Delta(\nu_{CC})$ vs. $\Delta G^{\ddagger}$ were investigated (Figure 4). The figure nicely shows the inverse relation between $\Delta G^{\ddagger}$ and $\Delta\delta$ and $\Delta\nu_{CC}$ which is due to the apparent anomaly in $\Delta\delta$ (vide supra). It also establishes that, despite the nonuniform changes between Fe/Ru and Ru/Os, there is a good linear relationship between these properties as the metal is changed. Clearly this implies that, as long as our assumption about the dependence of $\Delta G^{\ddagger}$ on metal–alkyne π-component is valid, at least in this class of compounds π-back-bonding also dominates changes affecting ν_{CC} and $\delta_{C_{alk}}$.

It is perhaps not totally unexpected that the small changes in $\Delta(\nu_{CC})$, $\Delta(\delta_{C_{alk}})$, and $\Delta G^{\ddagger}$ on going from Fe to Ru correspond also to the lesser stability of **2b** compared to that of **2a**. Similarly, $Ru(CO)_4(\eta^2$-olefin) compounds are less stable than their iron analogues.[3d] Discontinuity in stability at the second-row transition metal is not confined to the Fe triad but appears to be a general phenomenon for metal π-complexes. For instance, Maitlis et al.[39] found that in the series of complexes $(Ph_3P)_2M(\eta^2$-$CF_3C_2CF_3)$, the stability decreased in the order Pt > Ni > Pd. Moreover, for this class of alkyne–transition-metal derivatives the variation in $\Delta(\nu_{CC})$, Pt > Ni > Pd, reflects exactly the stability sequence and implies that with these highly basic d^{10} $M(PPh_3)_2$ fragments metal d to π^*(alkyne) back-bonding dominates the metal–alkyne interactions. This is clearly not the case with $M(CO)_4(\eta^2$-BTMSA) compounds. Here, due to the presence of the electron acceptor $M(CO)_4$ metal carbonyl fragment and the electron-rich bis(trimethylsilyl)acetylene, both σ- and π-components of the metal–alkyne interaction appear to play an important role in determining the overall thermodynamic stability of the bond.

Acknowledgment. We wish to thank the Natural Sciences and Engineering Research Council of Canada and the University of Alberta for financial support of this work and Johnson Matthey for generous loan of osmium tetraoxide.

Registry No. **1b**, 15696-40-9; **1c**, 15243-33-1; ^{13}CO-enriched **2a**, 109088-06-4; **2b**, 109088-05-3; ^{13}CO-enriched **2b**, 109088-07-5; **2c**, 109088-04-2; BTMSA, 14630-40-1; $Fe(^{13}CO)_5$, 16997-09-4; $Ru_3(^{13}CO)_{12}$, 104469-63-8.

Supplementary Material Available: Tables of anisotropic thermal parameters for non-hydrogen atoms and derived positional and thermal parameters for the hydrogen atoms for **2c** (2 pages); a listing of observed and calculated structure amplitudes for **2c** (12 pages). Ordering information is given on any current masthead page.

Trans Insertion of Activated, Symmetrically Disubstituted Acetylenes into the Metal–Hydrogen Bond of Bis(cyclopentadienyl)metal Hydrides of Rhenium, Tungsten, and Molybdenum

Gerhard E. Herberich* and Wilhelm Barlage

Institut für Anorganische Chemie, Technische Hochschule Aachen, D-5100 Aachen, FRG

Received January 16, 1987

The insertion reactions of Cp_2ReH and Cp_2WH_2 with $MeO_2CC{\equiv}CCO_2Me$ were reinvestigated. The kinetically controlled products are $Cp_2M[\eta^1$-(Z)-$C(CO_2Me){=}CH(CO_2Me)]$ (M = Re, **1a**; M = WH, **2a**) which can thermally isomerize to the more stable E isomers (M = Re, **1b**; M = WH, **2b**). Cp_2ReH inserts $NCC{\equiv}CCN$ to form $Cp_2Re[\eta^1$-(Z)-$C(CN){=}CH(CN)]$ (**5a**). Upon irradiation **5a** gives a photostationary mixture of **5a** and the E isomer **5b** (ratio 1:2). Pure **5b** thermally reverts to **5a** in the dark while irradiation affords the same isomeric mixture as above. The crystal structures of **1a** and **1b** were determined. For **1a**: space group $P2_1/c$ (No. 14), a = 915.5 (3) pm, b = 764.9 (2) pm, c = 2085.5 (1) pm, β = 92.10 (1)°, Z = 4; R = 0.041, R_w = 0.050. For **1b**: space group $P2_1/c$ (No. 14), a = 2169.5 (9) pm, b = 888.1 (1) pm, c = 1683.1 (8) pm, β = 111.36 (3)°, Z = 8; R = 0.042, R_w = 0.047. **2a** shows rotational isomerism about the metal–alkenyl bond with $\Delta G^{\ddagger}$ = 62.8 ± 0.5 kJ/mol at 298 K. The stereochemistry of the alkenyl group can be determined from the $^3J(^{13}C$–$^1H)$ coupling constants. For the Z isomers (e.g., **1a** and **5a**) the cis coupling constant ranges from 8.5 to 10 Hz while the trans constants of the E isomers (e.g., **1b** and **5b**) lie between 14 and 16 Hz.

Introduction

The insertion of acetylenes into metal–hydrogen bonds represents one of the fundamental processes of organometallic chemistry.[1-4] Insertion reactions may proceed in a cis or a trans manner.[2-4] This is exemplified in eq 1 for the most simple case of symmetrical disubstituted acetylenes which may give alkenyl complexes of Z or E stereochemistry. Several authors have pointed out that the determination of the product stereochemistry is not trivial.[2,5,6] Furthermore, the reaction stereochemistry can

(1) Collman, J. P.; Hegedus, L. S. *Principles and Applications of Organotransition Metal Chemistry*; University Science Books: Mill Valley, CA, 1980.
(2) Otsuka, S.; Nakamura A. *Adv. Organomet. Chem.* **1976**, *14*, 245.
(3) For a recent review of the literature see: Barlage, W. Dissertation, Technical University of Aachen, 1985.
(4) Bianchini, C.; Innocenti, P.; Masi, D.; Meli, A.; Sabat, M. *Organometallics* **1986**, *5*, 72. Amaudrut, J.; Leblanc, J.-C.; Moïse, C.; Sala-Pala, J. *J. Organomet. Chem.* **1985**, *295*, 167.

0276-7333/87/2306-1924$01.50/0